

In-plane backward and Zero-Group-Velocity guided modes in rigid and soft strips

Jérôme Laurent, Daniel Royer, and Claire Prada*
 ESPCI Paris, PSL Research University, CNRS, Institut Langevin,
 UMR 7587, 1 rue Jussieu, F-75005 Paris, France
 (Dated: December 11, 2021)

Elastic waves guided along bars of rectangular cross section exhibit complex dispersion. This paper studies in-plane modes propagating at low frequencies in thin isotropic rectangular waveguides through experiments and numerical simulations. These modes result from the coupling at the edge between the first order shear horizontal mode SH_0 of phase velocity equal to the shear velocity V_T and the first order symmetrical Lamb mode S_0 of phase velocity equal to the plate velocity V_P . In the low frequency domain, the dispersion curves of these modes are close to those of Lamb modes propagating in plates of bulk wave velocities V_P and V_T . The dispersion curves of backward modes and the associated ZGV resonances are measured in a metal tape using non-contact laser ultrasonic techniques. Numerical calculations of in-plane modes in a soft ribbon of Poisson's ratio $\nu \approx 0.5$ confirm that, due to very low shear velocity, backward waves and zero group velocity modes exist at frequencies that are hundreds of times lower than ZGV resonances in metal tapes of the same geometry. The results are compared to theoretical dispersion curves calculated using the method provided in Krushynska and Meleshko (*J. Acoust. Soc. Am* **129**, 2011).

I. INTRODUCTION

Early studies on the propagation of elastic waves in thin elongated strips were motivated by the need for long time ultrasonic delay lines. Today, rectangular elastic waveguides are encountered in miscellaneous contexts at different scales, from civil engineering structures to cantilever, micro-electromechanical systems (MEMS), or even in nanotechnology.^{1,2} Thin elastic waves guides are also present in biological systems as for example, tendons and ligaments in the musculoskeletal system³ or the basilar and the tectorial membranes in the cochlea.⁴ Elastic waves propagation in these elongated structures is quite complex, several modes can propagate with interesting dispersion properties that strongly depend on the material Poisson's ratio. In particular, some modes exhibit negative dispersion.

The existence of backward elastic modes propagating in homogeneous waveguides is well known and has been put in evidence in the past century.⁵ Experimental observations of these modes were first reported in wires^{6,7} and then for plates.⁸ At the minimum frequency of a backward mode, the resonance associated to the zero group velocity (ZGV) mode was pointed out by Tolstoy and Usdin⁹ and observed by Holland and Chimenti using air coupled transducers.¹⁰ Then non-contact laser ultrasonic techniques allowed precise measurements and thorough analysis of these modes in metal plates,^{11–14} but also in circular hollow cylinders^{15,16} and rods.¹⁷

While elastic guided modes in isotropic plates and circular cylinders are well described by an analytical formulation of the dispersion equations, the theory of elastic rectangular waveguides is much more complex. Indeed, the modes cannot be expressed in a closed form, except for some particular width-to-thickness ratio that were determined by Mindlin and Fox.¹⁸ Since the seminal work of Morse,¹⁹ several low frequencies approximations were proposed, for example, Medick used a one dimensional quadratic approximation allowing the calculation of the first eight breathing modes.²⁰ More recently, several studies based on numerical simulations using finite and boundary element methods provided ap-

proximate dispersion curves.^{21–26} A complete review of the theory can be found in the papers by Meleshko and Krushynska^{27,28} where the dispersion equations of rectangular elastic bars are formulated as infinite series and normal modes are studied for various width to thickness ratio and material parameters. The existence of several backward modes for Poisson's ratio up to 0.5 was pointed out for bars of width-to-thickness ratio higher than 5 in the study by Krushynska *et al.* (section III of paper²⁸).

In addition to these theoretical studies, the large majority of experimental results found in the literature deals with flexural modes at low frequencies. Seventy years ago, Morse measured dispersion curve on bars of different width-to-thickness ratios and compared them with low frequency approximation.²⁹ Twenty years later, the dispersion curves of higher order modes including backward modes were measured by Hertelendy in a square bar of an aluminum alloy.³⁰ More recently, several dispersion curves were measured in wooden bars by Veres *et al.* using laser interferometry and then compared to numerical simulations of a wooden orthotropic beam.³¹ Lately, Serey *et al.* addressed the selective generation of pure guided waves in an thin metal bar of rectangular cross-section using three component interferometry and an array of transducers, in a frequency range below the shear cut-off frequency.³² They were able to detect and generate modes with dominant out of plane displacement corresponding to edge reflections of the A_0 Lamb mode. In picosecond acoustics, Jean *et al.* have measured elastic resonances and a backward mode in gold nano-beam of rectangular cross section (370-nm wide and 110-nm thick). With semi-analytical finite element simulations (SAFE), the backward wave was identified as the first dilatational mode.² Very few studies report on measurements of in-planes modes. Cegla *et al.* detected shear horizontal mode propagating in a steel tape with a dual laser probe at frequency far above the shear cut-off frequency where the mode is non-dispersive and propagates at the shear wave velocity.²⁵ In-plane guided waves were also observed by Sellon *et al.* in ex-vivo tectorial membranes using optical means.⁴

In the present paper, we consider the low frequency in-plane modes propagating in thin rectangular bars. We study the corresponding backward mode and associated ZGV resonances for metal tapes as well as soft ribbons. The low frequency in-plane guided modes of rectangular tapes are described in section II. The dispersion curves are calculated for a metal and a soft strip following Krushynska *et al.*²⁸ and compared to the corresponding Rayleigh-Lamb (RL) modes approximation. In section III, ZGV resonances and dispersion curves of in-plane modes measured using laser ultrasonic techniques are presented and compared to the theory. In the last section IV, comparison between modes propagating in hard and soft ribbons is achieved through numerical simulations.

II. IN-PLANE MODES OF A THIN RECTANGULAR BEAM

At low frequencies, an isotropic plate supports the propagation of only three modes : the shear horizontal mode SH_0 , the compressional symmetric S_0 and the flexural antisymmetric A_0 Lamb modes. The symmetrical SH_0 and S_0 modes are both in-plane and non-dispersive: while the phase velocity of SH_0 is the shear velocity V_T , the S_0 phase velocity is approximated by the plate velocity V_P expressed from the bulk velocities V_L and V_T , as

$$V_P = 2V_T \sqrt{1 - \frac{V_T^2}{V_L^2}}. \quad (1)$$

This approximation is valid for frequencies f smaller than the first shear cut-off frequency $V_T/(2d)$, where d is the plate thickness.³³

If the plate is bounded in the transverse dimension, thus forming a rectangular waveguide of width $b \gg d$, then the in-plane modes SH_0 and S_0 are coupled through reflections at the edges (Fig. 1). As shown by Morse¹⁹ and by Medick and Pao,³⁴ this coupling is very similar to the one of shear and compressional bulk waves in a plate. The resulting guided modes have dispersion curves close to those of Lamb modes in a plate of thickness b and of bulk wave velocities V_P and V_T which corresponds to a material of Poisson's ratio

$$\nu' = \frac{\nu}{1 + \nu}, \quad (2)$$

where ν is the Poisson's ratio of the beam material.

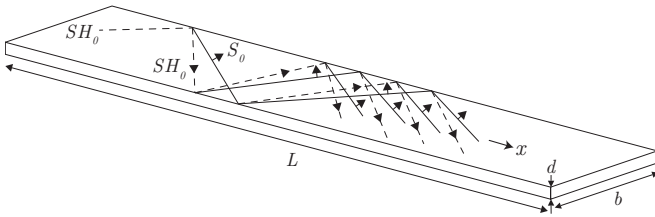


FIG. 1. In-plane modes conversion in a thin rectangular beam.

The calculation of guided modes in a rectangular waveguide²⁸ is described in Krushynska *et al.* Like in

the earlier paper by Fraser,³⁵ the modes are classified in four families depending on the displacement symmetries: the longitudinal L -modes, the torsional T -modes, the bending B_x -modes and B_y -modes. For thin beams with the smallest dimension along y -axis, the symmetrical in-plane S' -modes correspond to the longitudinal L -modes and the anti-symmetrical in-plane A' -modes to the bending B_x -modes. In Krushynska *et al.*,²⁸ the low frequency approximation of in-plane modes was confirmed for a plate of width to thickness ratio $b/d = 5$ and of Poisson's ratio $\nu = 1/4$, and for frequencies up to four times the first cut-off frequency $V_T/(2b)$.

The first symmetrical mode, here denoted S'_0 , is non dispersive below the first cut-off frequency and has a phase velocity V'_P slightly lower than the plate velocity V_P and equal to

$$V'_P = 2V_T \sqrt{1 - \frac{V_T^2}{V_P^2}}. \quad (3)$$

Using the plate to shear velocity ratio

$$\frac{V_P}{V_T} = \sqrt{\frac{2}{1 - \nu}} = \sqrt{\frac{2(1 - \nu')}{1 - 2\nu'}}, \quad (4)$$

a remarkably simple formulation of the pseudo-plate velocity to shear velocity ratio is obtained

$$\frac{V'_P}{V_T} = \sqrt{\frac{2}{1 - \nu'}} = \sqrt{2(1 + \nu)}. \quad (5)$$

In fact, the velocity V'_P is the bar velocity $\sqrt{E/\rho}$, which is the velocity of the low frequency longitudinal mode in an elastic guide of finite cross-section as established by Lord Rayleigh.³⁶ Noteworthy simple expressions of the velocities are found for two particular cases. For $\nu = 1/3$ the plate velocity is $V_P = \sqrt{3}V_T$ then $\nu' = 1/4$ and the velocity of the S'_0 mode at low frequencies is $V'_P = \sqrt{8/9}V_P \approx 0.94V_P$. For soft materials ν approaches 0.5, the plate velocity is $V_P = 2V_T$ which is much smaller than the longitudinal velocity.³⁷ Thus, in soft ribbon the bar velocity is $V'_P = \sqrt{3}V_T$. These remarkable parameters are gathered in Table I.

TABLE I. Remarkable plate and bar velocities.

Material	ν	ν'	V_P	V'_P
Metal	$\frac{1}{3}$	$\frac{1}{4}$	$\sqrt{3}V_T$	$\sqrt{\frac{8}{3}}V_T$
Soft	$\frac{1}{2}$	$\frac{1}{3}$	$2V_T$	$\sqrt{3}V_T$

Here, using the Meleshko Krushynska (MK) model,²⁸ theoretical dispersion curves are calculated for a Duraluminum tape of thickness $d = 2$ mm, width $b = 30$ mm and bulk velocities $V_L = 6400$ m/s, $V_T = 3140$ m/s. In Figure 2(a), the normalized frequency fb/V_T is represented as a function of the dimensionless wave number kb . Lamb modes in a plate of bulk velocities V_T and V_P and thickness b are also displayed for comparison. A very good agreement with the Lamb modes approximation is observed for frequencies up to $f = 4V_T/b$. As in a plate, several backward and ZGV modes exist. They occur when a shear (or SH_0)

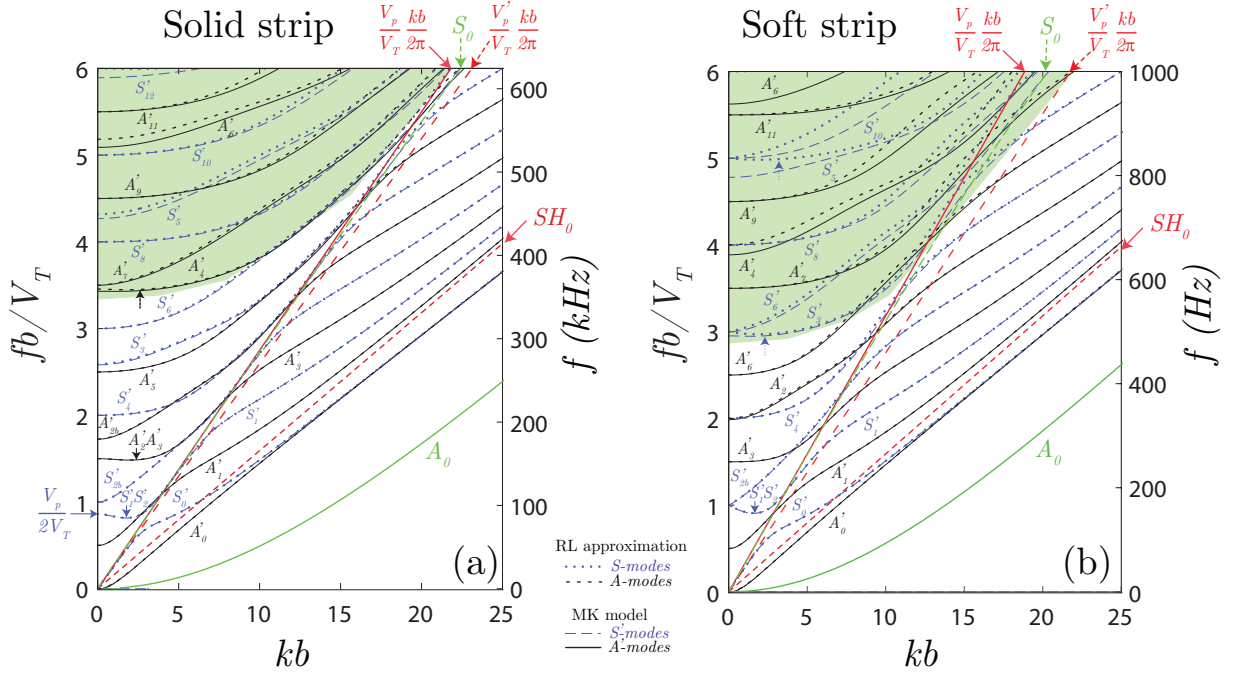


FIG. 2. In-plane modes dispersion curves calculated with MK-model for solid and soft strips of width $b = 30$ mm, thickness $d = 2$ mm and Poisson's ratio ν , compared to the Rayleigh-Lamb modes for a plate of thickness b and Poisson's ratio $\nu' = \nu/(1 + \nu)$. Thick red, blue and green solid lines are the first two Lamb modes and the first shear mode of a plate of thickness d and Poisson's ratio ν ; the red dashed line indicates the plate velocity. (a) Duraluminum tape of Poisson's ratio $\nu = 0.34$, (b) soft ribbon of bulk wave velocities $V_L = 1500$ m/s and $V_T = 5$ m/s. The cut-off frequency of S'_1 mode is $fb = V_T$. The S_0 mode coincides with the straight line $2\pi f = V_P k$ while the S'_0 mode is close to the line $2\pi f = V'_P k$ for $fb < 0.4V_T$.

cut-off frequency nV_T/b is close to a plate mode (or S_0) cut-off frequency mV_P/b of the same symmetry. $S'_1S'_2$ - and $A'_2A'_3$ -ZGV points are found at frequency wave number $(fb/V_T, kb) = (0.824, 1.77)$ and $(1.49, 1.95)$ respectively [Figure 2(a)]. The thick solid lines represent the first modes A_0 , S_0 , and SH_0 of an unbounded plate of thickness d . For higher frequencies, between A_0 and SH_0 modes, the A'_0 and S'_0 modes converge towards the edge or pseudo-Rayleigh mode.

While in plates, the S_1S_2 -ZGV Lamb mode only exists for Poisson's ratio below 0.451,³⁸ in thin rectangular beams, the $S'_1S'_2$ -ZGV mode exists for any Poisson's ratio. The behaviour of in-plane modes is particularly interesting in the case of soft material. Indeed, for $\nu \approx 0.5$, the plate velocity V_P is equal to $2V_T$ which results in a Dirac cone at the frequency $f = V_T/b$ as it happens for Lamb modes in a plate of Poisson's ratio $\nu = 1/3$.^{5,39,40} This is illustrated in Figure 2(b) displaying the in-plane mode dispersion curves for a 2 mm thick and 20 mm wide tape of velocities $V_L = 1500$ m/s and $V_T = 5$ m/s ($\nu = 0.4998$). Such low shear velocity corresponds to typical velocities measured in agar gel or soft tissues. The second SH_0 cut-off frequency coincides with the first S_0 cut-off frequency $f = V_P/(2b)$ and the repulsion between the branches S'_1 and S'_2 results in a 8% relative bandwidth S'_{2b} backward branch (from 230 to 249 Hz in the presented case). For both branches, the group velocity remains finite as $k \rightarrow 0$ and converges to $V_g = 2V_T/\pi$.⁵ The $S'_1S'_2$ -ZGV mode occurs at a frequency \times width product $fb = 4.53$ kHz.mm which is more than two orders of mag-

nitude lower than the frequency \times width product of the same ZGV mode in a metal tape $fb = 2.64$ MHz.mm.

As for plates or cylinders, the existence of ZGV modes depends on the material elastic parameters. For isotropic thin rectangular beams, this dependence is illustrated in Figure 3(a) displaying cut-off and ZGV resonance frequencies versus Poisson's ratio. Horizontal and increasing curved thin lines corresponds to SH_0 and S_0 width resonances, respectively. It appears that, while the $S'_1S'_2$ -ZGV mode exists for all Poisson's ratio, the $A'_1A'_2$ -ZGV mode exists for Poisson's ratio ν up to 0.47. Using the approach proposed in Clorennec *et al.* for plates,¹⁵ the resonance parameter β'_1 is defined as the ratio of the $S'_1S'_2$ -ZGV frequency to the first S_0 cut-off frequency $V_P/(2b)$ and β'_2 is defined as the ratio of $A'_1A'_2$ -ZGV frequency to the third SH_0 cut-off frequency $3V_T/(2b)$. There is a one-to-one correspondence between ratio of the first two ZGV resonances $3\beta'_2V_T/(\beta'_1V_P)$ and the Poisson's ratio [Figure 3(a)]. As a consequence and similarly to plates, the measurement of the first two local resonances provides the material Poisson's ratio of the rectangular tape.

III. MEASUREMENTS ON A METAL TAPE

In-plane guided modes are observed on metal strips using non-contact laser ultrasonic techniques. A Q-switched Nd:YAG (Yttrium Aluminium Garnet) laser providing 8-ns pulses of 10-mJ energy at a 8-Hz repetition rate (Quantel Centurion) is used as a thermoelastic source. The laser beam of diameter 2.5 mm is focused

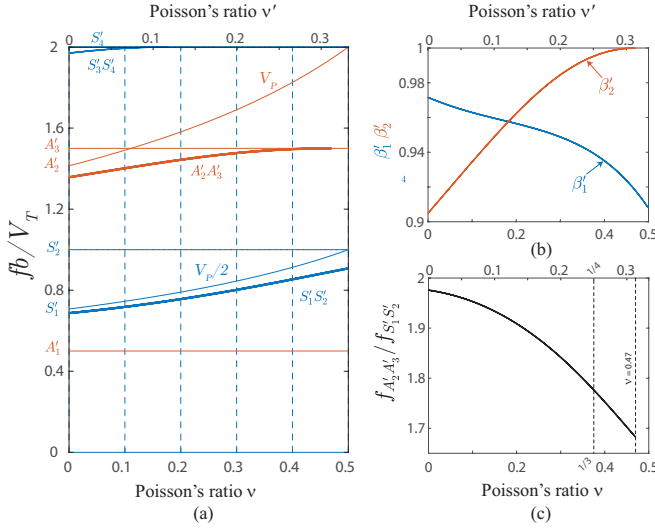


FIG. 3. In-plane modes of a thin ribbon: (a) Normalized cut-off (thin lines) and ZGV frequencies (thick lines) as a function of the material Poisson's ratio; the thin horizontal lines correspond to SH_0 cut-off frequencies, (b) Variations of the resonance parameters β'_1 and β'_2 versus Poisson's ratio, (c) Ratio between $A'_2A'_3$ - and $S'_1S'_2$ -ZGV frequencies.

into a narrow line with a beam expander ($\times 4$) and a cylindrical lens (focal length 250 mm). The full length of the source at $1/e$ of the maximum value was found to be 10 mm and the width was estimated to be 0.3 mm. With this features, the absorbed power density was below the ablation threshold. The source length is smaller than the optimal length to generate a ZGV mode but reasonable to generate several in-plane modes.⁴¹

In order to generate modes with symmetrical displacement component u_z , the line source was located in the middle of the tape edge (plane $z = 0$). Then, to detect in-plane modes, the normal surface displacement u_y was measured on the opposite edge with a heterodyne interferometer equipped with a 100-mW frequency doubled Nd:YAG laser (optical wavelength $\Lambda = 532$ nm) [Fig. 4(a)].

First measurements were done on a 1-m long Duraluminum tape of thickness $d = 0.5$ mm and width $b = 20$ mm. A significant displacement is detected for more than 3 ms after the laser impact Fig. 4(b). This duration is mostly due to the reflections at the tape ends of edge modes similar to those measured by Jia *et al.*⁴² During the first 100 μ s (inset) a typical waveform is observed with the first arrival of the compressional mode S_0 , followed by the first arrival of the shear mode SH_0 , as well as a low frequency resonance. The Fourier transform displayed in Fig. 4(c) highlights the first two ZGV resonances: $S'_1S'_2$ at 0.127 MHz and $A'_2A'_3$ at 0.227 MHz.

Similar measurements were also performed on two $d = 2$ mm thick tapes of width $b = 25$ or 30 mm. Normalized spectrum are displayed in Fig. 5(a). For the three tapes, the local resonance frequencies correspond to the theoretical $S'_1S'_2$ - and $A'_2A'_3$ -ZGV resonances frequencies calculated for a material of Poisson's ratio $\nu = 0.332$ [Fig. 5(b)] which is in good agreement with values generally found in the literature for aluminum alloys.

In order to confirm the origin of the resonances, the source was translated along the strip over 350 mm to observe the different modes. A Bscan $u_y(x, t)$ was recorded during 3 ms [Fig. 6(a)]. The signal is dominated by the pseudo-Rayleigh waves (edge wave) and the first reflections at the tape end appear after 400 μ s. An average of 2D-Fourier transforms calculated on 450 μ s sliding time windows provides the dispersion curves. Several modes are measured up to a frequency \times width product of $fb = 4V_T$. The $S'_1S'_2$ - and $A'_2A'_3$ -ZGV points just below the cut-off frequencies $fb = V_T$ and $fb = 1.5V_T$ as well as the associated backward modes are clearly identified and in good agreement with theoretical curves. The temporal Fourier transform of the displacement profile $u_y(x, f)$ is displayed around the $S'_1S'_2$ -ZGV frequency (Fig. 7). The interference pattern of the ZGV modes is clearly observed at $f = 84.85$ kHz and shown in the top figure. The red dashed line is the damped cosine function $|\cos(2\pi x/\lambda_{S'_1S'_2})| \times \exp(-\alpha|x|)$ where the ZGV mode wavelength is $\lambda_{S'_1S'_2} = 103$ mm and α is an adjusted damping parameter. This profile is in good agreement with the numerical displacements field that will be shown in the appendix.

IV. HARD AND SOFT RIBBON: COMPARISON THROUGH NUMERICAL ANALYSIS

In order to complete these measurements, the finite-difference time domain code Simsonic⁴³ was used to simulate the propagation of low frequency in-plane modes in a thin tape. The first calculation was achieved for the Duraluminum tape similar to the one in the experiments ($L = 10$ m, $b = 30$ mm and $d = 2$ mm). Then, we calculated the waves propagating in a soft ribbon of Poisson's ratio $\nu \approx 0.5$ with $V_T = 5$ m/s, and $V_L = 1500$ m/s and of geometrical parameters $L = 2$ m, $b = 20$ mm and $d = 2$ mm. The strips lengths were chosen large enough to avoid mode reflections at the end.

In order to excite in-plane modes, a normal velocity source with a constant profile along the thickness and a Gaussian profile along the x -axis, was applied on one tape edge. Then the velocity field $V_y(t, x, b/2, 0)$ was registered along the opposite edge for $-1 < x < 1$ m, during 2 ms for the metal tape and 200 ms for the soft ribbon. It is represented as function of dimensionless time tV_T/b and distance x/b Fig. 8(a) and Fig. 8(d). In both Bscan, it can be observed that after two or three reflections of the S_0 mode, the stationary modes appear.

The 2D-Fourier transform of the field $V_y(t, x, b/2, 0)$, $x > 0$ is calculated and displayed with the theoretical dispersion curves calculated with the MK-model Fig. 8(b) and Fig. 8(e). The modes having a non-zero velocity component V_y are observed and are in good agreement with the theoretical ones. For the solid strip, the two backward modes S'_{2b} and A'_{2b} are clearly detected. In the soft strip, the well generated S'_{2b} backward mode appears as the continuation of the S'_2 mode, confirming the existence of a Dirac cone.

The frequency spectra of the velocity recorded at point $(x, y, z) = (0, -b/2, 0)$ opposite to the source center are plotted Fig. 8(c) and Fig. 8(f). For the solid strip, the three resonances are associated to the S_0 mode cut-off of

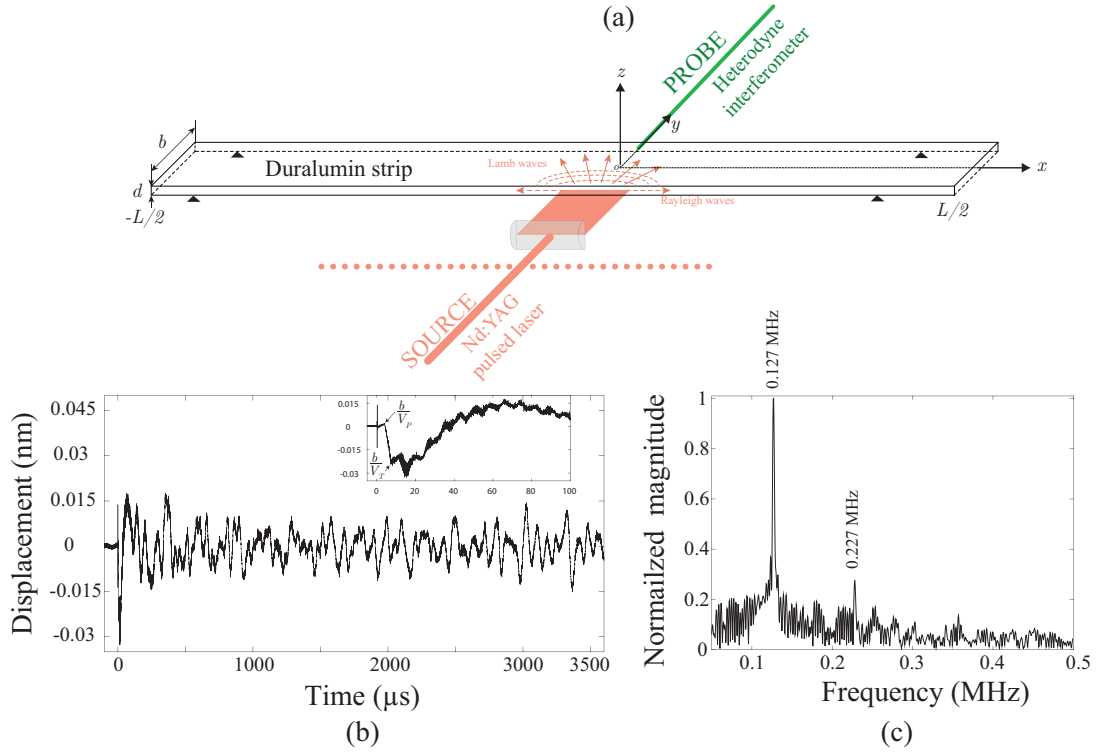


FIG. 4. (a) Schematic diagram of in-plane guided wave measurement in a metallic strip. The excitation is achieved on one edge with a laser line source parallel to the plate surface. The normal surface displacement is measured on the opposite edge with an interferometer, (b) Displacement measured at the epicentre on a strip of thickness $d = 0.5$ mm and width $b = 20$ mm, (c) Fourier transform of the first 200 μ s of the measured signal.

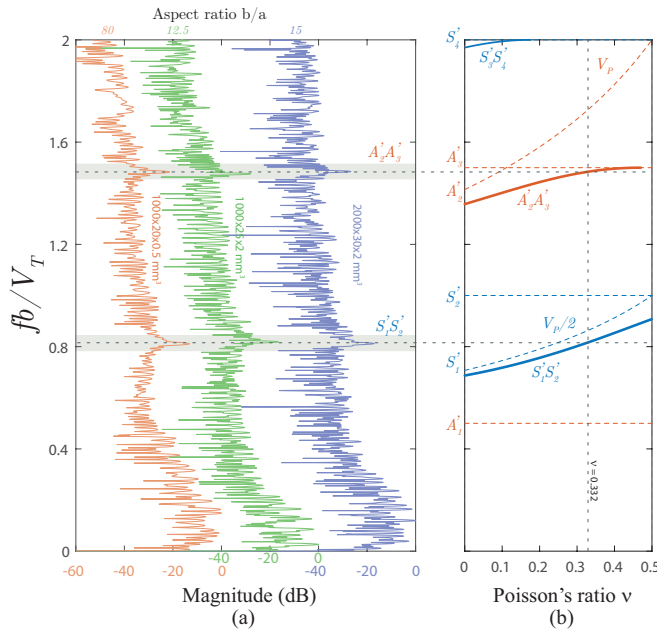


FIG. 5. (a) Local resonance spectrum measured on three Duraluminum tapes, (b) ZGV (solid lines) and cut-off (dashed lines) normalized resonance frequencies as a function of Poisson's ratio.

S'_{2b} , A'_2 and S'_3 , the other two are the $S'_1S'_2$ - and $A'_2A'_3$ -ZGV resonances that were measured in the experiment. The cut-off frequency resonances are well excited in this

numerical simulation because the source is normal to the edge, which is in favor the S_0 plate mode generation, while a laser source in the thermoelastic regime mostly generate a shear wave.⁴⁴ For the soft strip, the $S'_1S'_2$ - and $S'_3S'_6$ -ZGV resonances and the A'_2 cut-off resonance dominate. On the contrary, there is no significant resonance at the S'_2 (or S'_{2b}) cut-off frequency. In fact, as shown by Mindlin,⁵ at the Dirac cone the group velocity remains finite and is $V_g = 2V_T/\pi$ so that all modes are propagative and no resonance occurs.

V. CONCLUSION

The propagation of in-plane modes in thin rectangular beams, corresponding to low frequency longitudinal L -modes and bending B_x modes, was studied. Dispersion curves were simulated and measured in metallic tape. A good agreement was observed with theoretical dispersion curves calculated with the Meleshko-Krushynska (MK) model. The backward modes and the associated Zero-Group-Velocity mode resonances were clearly observed. We showed that these resonances do not depend on the strip thickness and that the measurement of the two lowest ZGV resonances can be used to determine the strip material Poisson's ratio ν . Non-dissipative soft ribbons were then considered, showing that backward modes exist at frequencies very low compared to the longitudinal cut-off frequency. These backward modes weakly coupled to the embedding fluid, could occur in the tectorial membrane for example and the associated

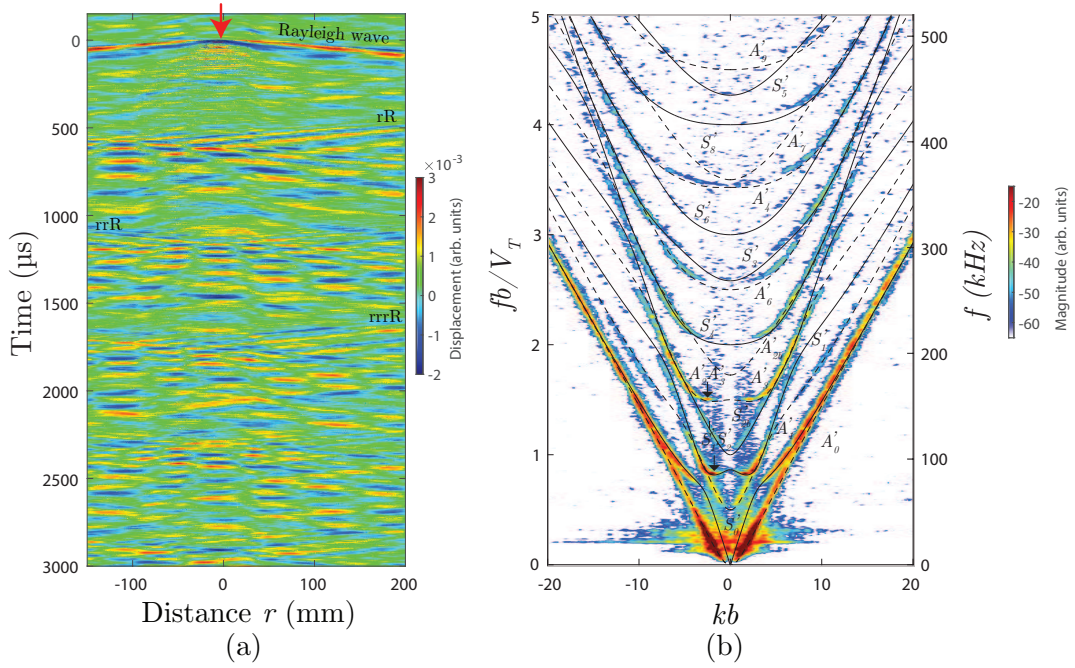


FIG. 6. (a) Displacement u_y measured along the edge of a Duraluminum tape of dimensions $L = 2$ m, $b = 30$ mm and $d = 2$ mm. (b) 2D-Fourier analysis of the displacement field with superimposed theoretical dispersion curves in black and red dashed lines.

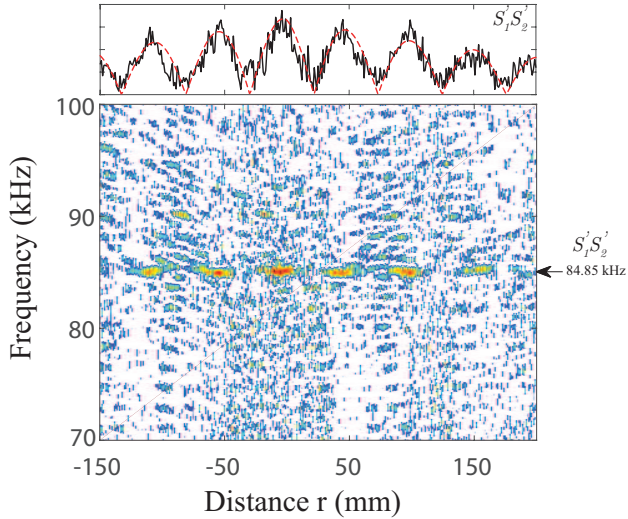


FIG. 7. Spatial distribution of the u_y measured displacement around the $S'_1S'_2$ -ZGV frequency. The top figure represents the amplitude profile at the frequency 84.85 kHz (black) and the theoretical damped cosine profile (red dashed line).

in-plane displacements may play a role in the complex audition mechanism. However, theoretical studies should be conducted to account for viscoelastic properties and new experiments should be developed to measure guided waves in soft strips.

ACKNOWLEDGEMENTS

The authors wish to thank B. Gérardin for drawing our attention on Santamore and Cross paper, and A.

A. Krushynska for fruitful discussions on dispersion curves in elastic bars of rectangular cross-section. They are grateful for funding provided by LABEX WIFI (Laboratory of Excellence within the French Program Investments for the Future, ANR-10-LABX-24) and ANR-10-IDEX-0001-02 PSL*.

APPENDIX

Appendix A1: Displacement field at ZGV resonance frequencies

For the Duraluminum, the velocity field (v_x, v_y) was also recorded in the plane $z = 0$ and the in-plane displacement field deduced by numerical integration. After temporal Fourier transform of 1 ms signal, the in-plane displacement distribution was observed at the first two ZGV frequencies [Figs. A1(a)-A1(d)]. The displacement components u_x and u_y are of the same order of magnitude and similar to those of ZGV Lamb modes.¹²

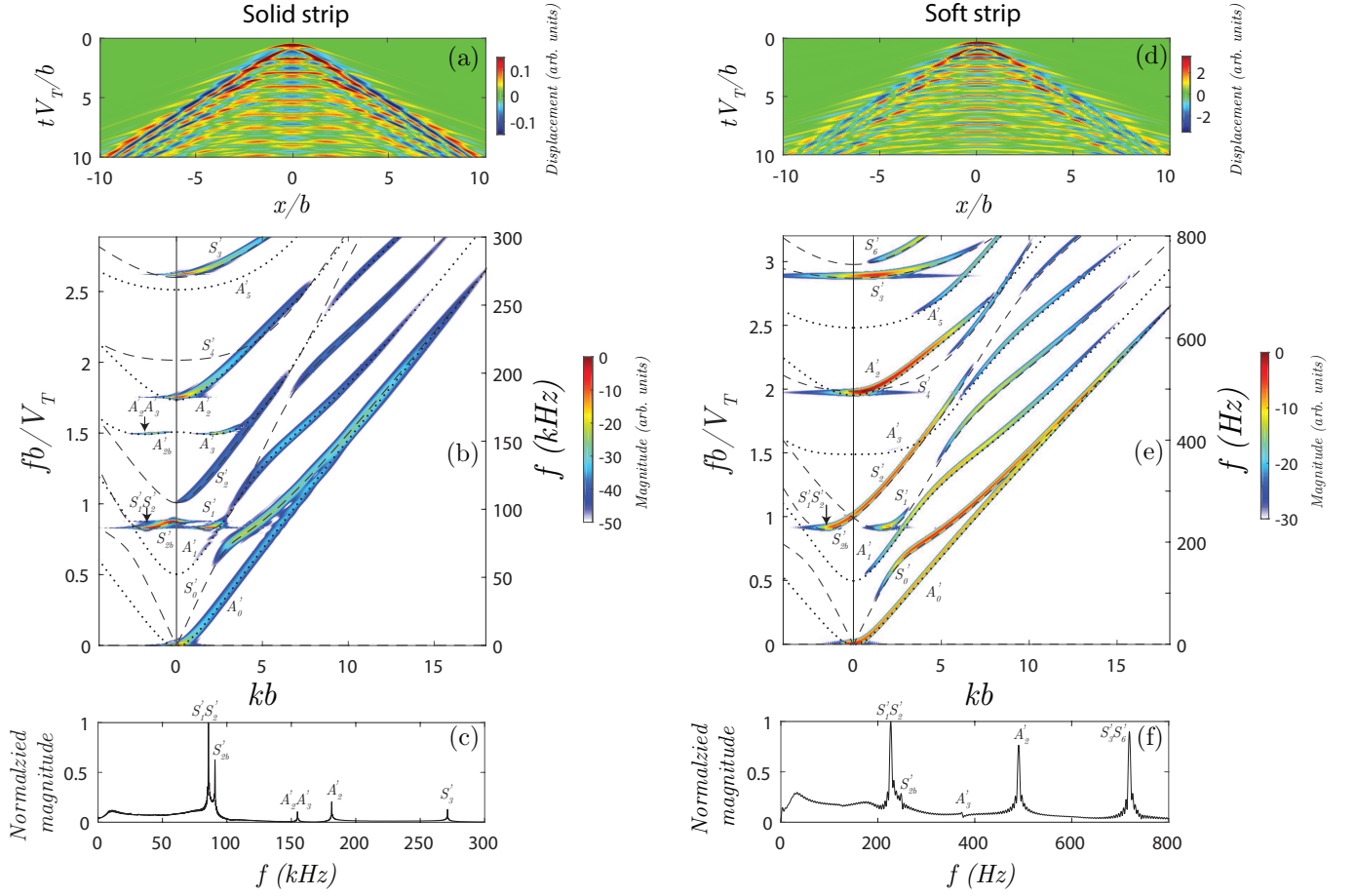


FIG. 8. Simulated in-plane mode propagation in a Duraluminum tape of parameters $L = 10$ m, $b = 30$ mm, $d = 2$ mm, $V_L = 6400$ m/s, $V_T = 3140$ m/s (left) and a soft ribbon of parameters $L = 2$ m, $b = 20$ mm, $d = 2$ mm, $V_L = 1500$ m/s, $V_T = 5$ m/s (right): normal edge velocity as a function of dimensionless time and distance (a) and (d); 2D-Fourier transform of the normal edge velocity with superimposed theoretical dispersion curves obtained with MK model (b) and (e); local resonances recorded at point $(x, y, z) = (0, -b/2, 0)$ opposite to the source center (c) and (f).

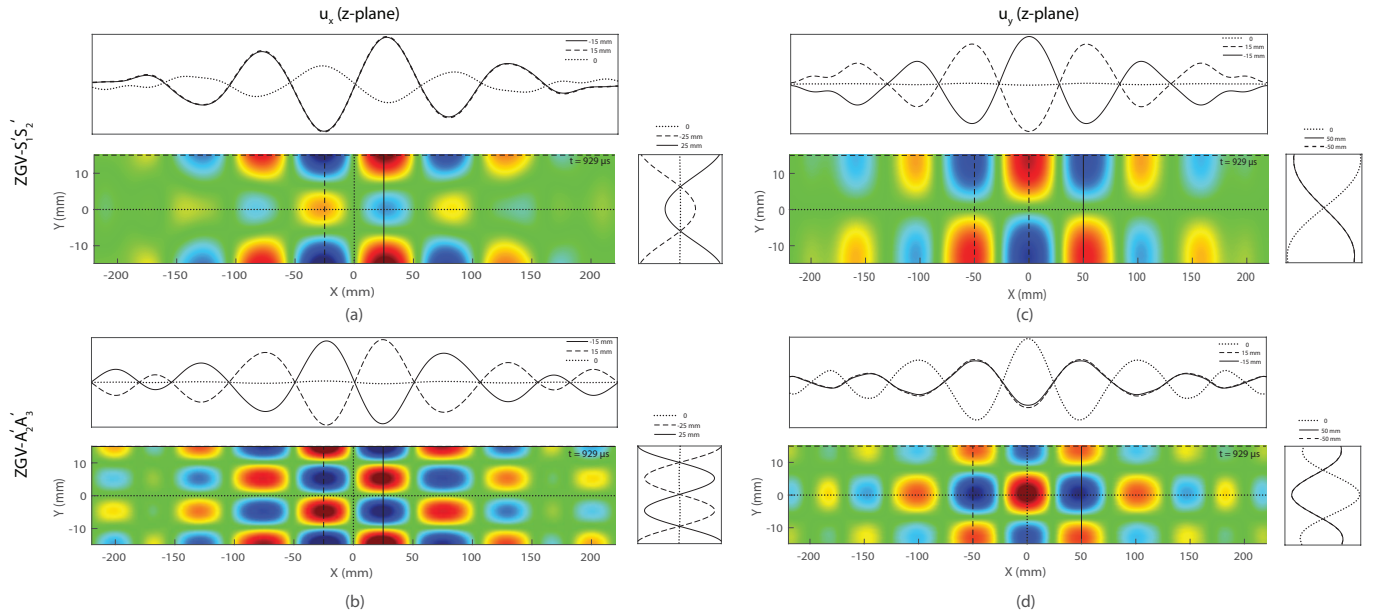


FIG. A1. In-plane displacement components at the $S_1'S_2'$ -ZGV frequency u_x (a) and u_y (c) and at the $A_2'A_3'$ -ZGV frequency u_x (b) and u_y (d) simulated with the elastodynamic FDTD code Simsonic for a Duraluminum tape of aspect ratio $b/d = 15$.

- * claire.prada@espci.fr
- ¹ D. H. Santamore and M. C. Cross, “Surface scattering analysis of phonon transport in the quantum limit using an elastic model”, *Phys. Rev. B*, **66**, 144302 (2002).
 - ² C. Jean, L. Belliard, L. Becerra, and B. Perrin, “Backward propagating acoustic waves in single gold nanobeams”, *Appl. Phys. Lett.* **107**, 193103 (2015).
 - ³ J. Brum, M. Bernal, J. Gennisson, and M. Tanter, “In vivo evaluation of the elastic anisotropy of the human Achilles tendon using shear wave dispersion analysis”, *Phys. Med. Biol.* **59**, 505 (2014).
 - ⁴ J. B. Sellon, S. Farrahi, R. Ghaffari, and D. M. Freeman, “Longitudinal spread of mechanical excitation through tectorial membrane traveling waves”, *Proc. Natl. Ac. Sci.* **112**, 12968–12973 (2015).
 - ⁵ R. D. Mindlin, *An introduction to the mathematical theory of vibrations of elastic plates*, US army Signal Corps Eng. Lab. (1955).
R. D. Mindlin, *An introduction to the mathematical theory of vibrations of elastic plates.*, Singapore: World Scientific, Ed. J. Yang (2006).
 - ⁶ T. Meeker and A. Meitzler, “Guided wave propagation in elongated cylinders and plates”, *Phys. Acoust.* **1**, 111–167 (1964).
 - ⁷ A. Meitzler, “Backward-wave transmission of stress pulses in elastic cylinders and plates”, *J. Acoust. Soc. Am.* **38**, 835–840 (1965).
 - ⁸ J. Wolf, T. D. K. Ngoc, R. Kille, and W. G. Mayer, “Investigation of Lamb waves having a negative group velocity”, *J. Acoust. Soc. Am.* **83**, 122 (1988).
 - ⁹ I. Tolstoy and E. Usdin, “Wave propagation in elastic plates: low and high mode dispersion”, *J. Acoust. Soc. Am.* **29**, 37–42 (1957).
 - ¹⁰ D. Holland and D. E. Chimenti, “Air-coupled acoustic imaging with zero-group-velocity Lamb modes”, *Appl. Phys. Lett.* **83**, 2704–2706 (2003).
 - ¹¹ C. Prada, O. Balogun, and T. Murray, “Laser based ultrasonic generation and detection of Zero-Group Velocity Lamb waves in thin plates”, *Appl. Phys. Lett.* **87**, 194109 (2005).
 - ¹² O. Balogun, T. Murray, and C. Prada, “Simulation and Measurement of the optical excitation of the S1 zero group velocity Lamb wave resonance in plate”, *J. App. Phys.* **102**, 064914 (2007).
 - ¹³ D. Clorennec, C. Prada, D. Royer, and T. W. Murray, “Laser impulse generation and interferometer detection of Zero Group Velocity Lamb mode resonance”, *Appl. Phys. Lett.* **89**, 024101 (2006).
 - ¹⁴ C. Grünsteidl, T. W. Murray, T. Berer, and I. A. Veres, “Inverse characterization of plates using zero group velocity Lamb modes”, *Ultrasonics* **65**, 1–4 (2016).
 - ¹⁵ D. Clorennec, C. Prada, and D. Royer, “Local and non-contact measurements of bulk acoustic wave velocities in thin isotropic plates and shells using zero group velocity Lamb modes”, *J. Appl. Phys.* **101**, 034908 (2007).
 - ¹⁶ M. Cès, D. Clorennec, D. Royer, and C. Prada, “Thin layer thickness measurements by zero group velocity Lamb mode resonances”, *Rev. Sci. Instr.* **82** (2011).
 - ¹⁷ J. Laurent, D. Royer, and C. Prada, “Temporal behavior of laser induced elastic plate resonances”, *Wave Motion* **51**, 1011–1020 (2014).
 - ¹⁸ R. Mindlin and E. Fox, “Vibrations and waves in elastic bars of rectangular cross section”, *J. Appl. Mech.* **27**, 152–158 (1960).
 - ¹⁹ R. Morse, “The velocity of compressional waves in rods of rectangular cross section”, *J. Acoust. Soc. Am.* **22**, 219–223 (1950).
 - ²⁰ M. A. Medick, “Extensional waves in elastic bars of rectangular cross section”, *J. Acoust. Soc. Am.* **43**, 152–161 (1968).
 - ²¹ O. M. Mukdadi, Y. Desai, S. Datta, A. Shah, and A. Niklasson, “Elastic guided waves in a layered plate with rectangular cross section”, *J. Acoust. Soc. Am.* **112**, 1766–1779 (2002).
 - ²² O. M. Mukdadi and S. K. Datta, “Transient ultrasonic guided waves in layered plates with rectangular cross section”, *J. Appl. Phys.* **93**, 9360–9370 (2003).
 - ²³ N. Stephen and P. Wang, “Saint-Venant decay rates for the rectangular cross section rod”, *J. Appl. Mech.* **71**, 429–433 (2004).
 - ²⁴ D. H. Cortes, S. K. Datta, and O. M. Mukdadi, “Elastic guided wave propagation in a periodic array of multi-layered piezoelectric plates with finite cross-sections”, *Ultrasonics* **50**, 347–356 (2010).
 - ²⁵ F. Cegla, “Energy concentration at the center of large aspect ratio rectangular waveguides at high frequencies”, *J. Acoust. Soc. Am.* **123**, 4218–4226 (2008).
 - ²⁶ R. Kažys, E. Žukauskas, L. Mažeika, and R. Raišutis, “Propagation of Ultrasonic Shear Horizontal Waves in Rectangular Waveguides”, *Int. J. Struct. Stab. Dyn.* **16**, 1550041 (2016).
 - ²⁷ V. Meleshko, A. Bondarenko, A. Trofimchuk, and R. Abasov, “Elastic waveguides: history and the state of the art. II”, *J. Math. Sci.* **167**, 197–216 (2010).
 - ²⁸ A. Krushynska and V. Meleshko, “Normal waves in elastic bars of rectangular cross section”, *J. Acoust. Soc. Am.* **129**, 1324–1335 (2011).
 - ²⁹ R. W. Morse, “Dispersion of compressional waves in isotropic rods of rectangular cross section”, *J. Acoust. Soc. Am.* **20**, 833–838 (1948).
 - ³⁰ P. Hertelendy, “An approximate theory governing symmetric motions of elastic rods of rectangular or square cross section”, *J. Appl. Mech.* **35**, 333–341 (1968).
 - ³¹ I. A. Veres and M. B. Sayir, “Wave propagation in a wooden bar”, *Ultrasonics* **42**, 495–499 (2004).
 - ³² V. Serey, N. Quaegebeur, P. Micheau, P. Masson, M. Castaings, and M. Renier, “Selective generation of ultrasonic guided waves in a bi-dimensional waveguide”, *Struct. Health Monit.* pages 1–13 (2018).
 - ³³ D. Royer and E. Dieulesaint, *Elastic Waves in Solids I: Free and Guided Propagation*, Springer (1999).
 - ³⁴ M. Medick and Y.-H. Pao, “Extensional vibrations of thin rectangular plates”, *J. Acoust. Soc. Am.* **37**, 59–65 (1965).
 - ³⁵ W. Fraser, “Stress wave propagation in rectangular bars”, *Int. J. Sol. Struct.* **5**, 379–397 (1969).
 - ³⁶ G. Kynch, “The fundamental modes of vibration of uniform beams for medium wavelengths”, *British J. Appl. Phys.* **8**, 64 (1957).
 - ³⁷ A. Sarvazyan, “Low-frequency acoustic characteristics of biological tissues”, *Poly. Mech.* **11**, 594 (1975).
 - ³⁸ C. Prada, D. Clorennec, and D. Royer, “Power law decay of Zero Group Velocity Lamb modes”, *Wave Motion* **45**, 723–728 (2008).
 - ³⁹ A. Maznev, “Dirac cone dispersion of acoustic waves in plates without phononic crystals”, *J. Acoust. Soc. Am.* **135**, 577–580 (2014).
 - ⁴⁰ D. M. Stobbe and T. W. Murray, “Conical dispersion of Lamb waves in elastic plates”, *Phys. Rev. B* **96**, 144101 (2017).
 - ⁴¹ Optimal source length at constant maximum surface energy density: The absorbed energy distribution is written as $E(x) = I \exp(-x^2/l^2)$ where I is supposed to be lower

than the ablation threshold. The resulting Fourier transform is given by $\mathbf{E}(k) = (I\sqrt{\pi}l) \times \exp(-l^2k^2/4)$. The amplitude of a mode of wave number k reaches a maximum for the optimal source length $l_{opt} = \lambda/(\pi\sqrt{2})$.

- ⁴² A. Jia, “Laser-generated pseudo-Rayleigh acoustic wave propagating along the edge of a thin plate”, *J. Appl. Phys.* **80**, 2595 (1996).

- ⁴³ E. Bossy, M. Talmant, and P. Laugier, “Three-dimensional simulations of ultrasonic axial transmission velocity measurement on cortical bone models”, *J. Acoust. Soc. Am.* **115**, 2314 (2004).
- ⁴⁴ D. Hutchins, R. Dewhurst, and S. Palmer, “Directivity patterns of laser-generated ultrasound in aluminum”, *J. Acoust. Soc. Am.* **70**, 1362–1369 (1981).